SUBDERMAL EEG MEASUREMENT SYSTEM FOR THE CONTROL OF A BIONIC HAND – PART 2

ELEN4006

School of Electrical & Information Engineering, University of the Witwatersrand, Private Bag 3, 2050, Johannesburg, South Africa

Joshua Schwark (2118091)

Submission Date: 6th May 2024

Abstract: This work presents a novel approach to addressing motor disabilities through the development of a measurement system utilising sub-dermal electroencephalogram electrodes for controlling bionic prosthetic hands in paralysed patients. The investigation delves into capturing, conditioning, and processing electroencephalogram signals to identify motor imagery tasks within a Brain Computer Interface. Signals from the UNEEG SubQ 24/7 sensor would undergo amplification, filtering, and processing to be useful to the Brain Computer Interface and presentation. A detailed description of the design is discussed including the components used. A performance evaluation and critical analysis is completed verify the design.

Key words: BCI, EEG, sensor, signal-conditioning, sub-scalp

1. INTRODUCTION

Brain-Computer Interfaces (BCIs) are a modern solution to challenges associated with motor disabilities by enabling communication between the brain and external prostheses [1]. This project's focus is on developing a measurement system utilising sub-dermal electroencephalogram (EEG) electrodes for controlling a bionic prosthetic hand. This system would be targeted at individuals who would not want to wear a large EEG headband and have a bigger budget. This system would capture and analyse EEG signals which are voltage waveforms [2]. These signals would be used to identify motor imagery tasks and would need to be conditioned and processed to ensure the signals can be used by the bionic hand. Individuals with motor disabilities or amputations face difficulties in controlling traditional prosthetic devices [3]. A method of control for bionic prostheses, Electromyographic (EMG) sensors, relies on muscle contractions, which would not be viable for a person with partial upper limb paralysis [3], highlighting the need for a more intuitive and efficient means of control. Using EEG technology, the proposed solution enables users to generate commands by simply imagining specific hand gestures, such as a fist closure [4]. This report discusses the design specifications and implementation of the EEG-based measurement system for bionic control. The subsequent sections will perform a detailed analysis, including an evaluation of components, quantification of the performance and a critical analysis.

2. DESIGN SPECIFICATION AND HIGH-LEVEL SOLUTION

Voltage waveforms would be obtained from the sub-dermal electrode on the C3 electrode to control the right hand [2]. The signal will go through two amplification stages to avoid high gains and therefore ensure gain remains constant through all frequencies under 100 Hz due to gain-bandwidth product. The first stage is through an instrumentation amplifier with a gain of 1000. This would take the signals from ± 200 µV to ±200 mV. The signal would then be filtered through a low pass filter at 99 Hz and a high pass filter as 0.5 Hz limiting the bandwidth to 98.5 Hz. Lastly the signal will go through a non-inverting summing amplifier to apply a DC shift to the signal to remove negative voltages and apply a final amplification of 12.5 times so that it is in the range of 0 to 5 V to be used by the Analog to Digital converter (ADC). A notch filter is implemented digitally on the microprocessor to reduce any noise induced due to mains power interference. A digital filter is easier to implement for higher orders with less roll-off. These specifications are summarised in Table 1.

Table 1: Table showing the Specifications of the Measurement System.

Specification	Variable	
Input voltage range	+/- 0-200 µV	[5]
Output voltage range	0V – 5V	
Bandwidth	0.5 Hz to 99 Hz (98.5 Hz)	[6]
Accuracy	± 10% error	[7]
Battery Life	+ 10 hours	
Sampling Frequency	+ 200 Hz	[6] [8]
IP rating	IP 64	

3. Detailed Design

The detailed design is specified below. A circuit diagram of the design is shown in the appendix showing the specific components used at each stage. Figure 1 below shows a flow diagram of the system.

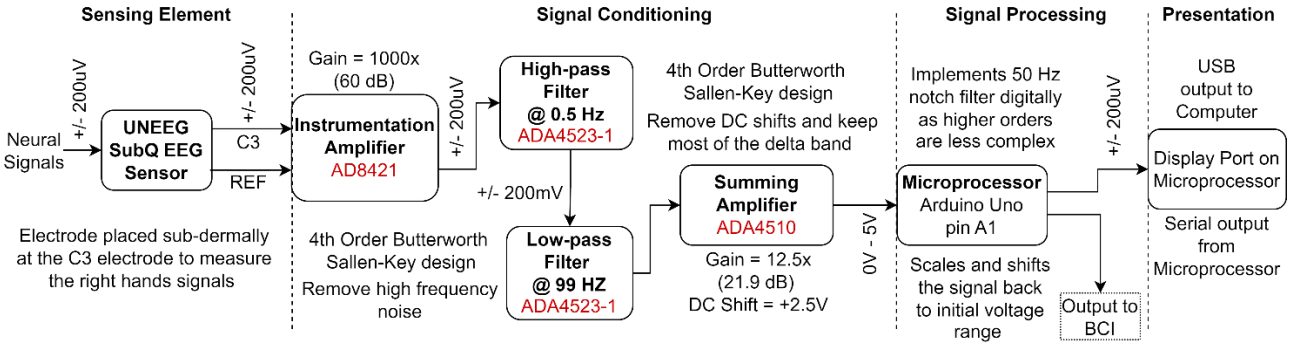

Figure 1: Flow diagram of the whole system.

3.1. Sensor Element

The UNEEG SubQ sensor is a sub-dermal EEG electrode [9]. This sensor is designed for long-term EEG monitoring and therefore certain aspects are adjusted for the specification of the design. This active electrode samples as 207 Hz and has a dynamic range of +350 µV. This sensor has a +10% accuracy at 50 µV for all frequencies within 1 Hz to 48 Hz. The electrode has a bandwidth of the full EEG bandwidth of 0.5 Hz to 100 Hz and it is assumed as sensorimotor signals can be found through the sensor's bandwidth range. This sensor will send a signal from the reference electrode and the C3 electrode in the range of -200 µV to 200 µV.

3.2. Signal Conditioning

The two signals from the reference and C3 electrodes are fed into an instrumentation amplifier (AD8421). This amplifier has a gain of 1000 times (60dB), and the outputted signal would be in the range of -200 mV to 200 mV. It is chosen due to its high precision and Common Mode Rejection Ratio [10]. DC offset is also adjusted from the reference node of the instrumentation amplifier. Due to this amplifier's high bandwidth of 1 MHz, the gain-bandwidth product would not be an issue. The output of the instrumentation amplifier has a buffer resistor to provide isolation and prevent loading effects and is sent to an active high pass filter with a cut-off frequency of 0.5 Hz and 80dB/dec roll-off and active low pass filter with a cut-off frequency of 99 Hz with 80dB/dec roll-off. Both filters are two stage 4th Order Butterworth filters with a Sallen-Key topology and use a ADA4523-1 amplifier. This amplifier is chosen for its low noise and zero drift features [11]. The filters are two stage to decrease the roll off and increase the order. Lastly, the signal is passed into a summing amplifier (ADA4510). This amplifier has a gain of 12.5 (21.9 dB) and would be summed with a DC gain of 2.5V to scale the signal. The output of this amplifier would be between 0 V and 5 V. The amplifier is chosen due to its high precision, low noise features [12]. This would result in an overall

gain of 81.9 dB or 12500 times for the system.

3.3. Signal Processing

The signal processing will be performed on an Arduino Uno. The microcontroller has an inbuilt analogue-to-digital converter (ADC). The ADC converts the signal to digital values. A digital notch filter will be implemented on the microcontroller as higher order filters with less roll off are easier to implement digitally. The voltage is amplified linearly throughout the system. This would allow for a shift of -2.5 V to be performed on the signal along with a scale of 1/12500 to allow the signal to be represented as equally to the input signal and undo the effects of the amplification. This would be needed for data presentation. To determine the sampling rate for the ADC that would avoid aliasing the sampling rate would need to be greater than the highest frequency that needs to be preserved. The Nyquist theorem says that the minimum limit for sampling should be twice the highest desired frequency. The highest desired frequency is 100 Hz and according to Nyquist the minimum sampling frequency would be 200 Hz. An Arduino Uno has an ADC clock speed of 125 kHz when maintaining 10-bit resolution as the ADC clock has two rest cycles, which surpasses the necessary sampling frequency and would be high enough to mitigate aliasing.

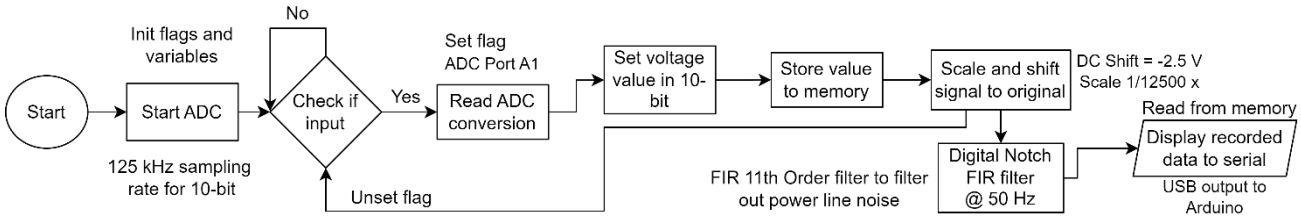

Figure 2: Microcontroller Logic Flow Diagram

3.4. Data Presentation

Data will be displayed through a port on the microcontroller. The USB output of the Arduino will be used to display the signal through the serial write command. This would then be displayed on the computer that the USB is plugged into. This would only be used to verify the inputted neural signals and bug testing.

3.5. Powering the circuit

The circuit will be powered with a 9 V Lithium-ion battery along with buck converters to supply the correct voltage to the rails of the operational amplifiers at 5 V and -5 V. The Arduino will be powered using the barrel power port directly from the 9 V battery. The battery has a capacity of 1000 mAh and is rechargeable via microUSB [13].

4. PERFORMANCE EVALUATION

Table 2 below shows the errors that are propagated through the system. These errors are all based on the voltages that go through each amplifier at the respective stage of the system. These errors would affect the voltage-time signal that is displayed and sent to the BCI. The total error of the system is calculated by the summation of each elements error. This would be a 10.50% error as shown in Table

2, which would result in a system accuracy of 89.50% The sensor has a maximum 10% error [9], with no noted temperature variations. Error induced due to the op-amps would be gain error in the instrumentation amplifier and Offset voltage and offset voltage drift in the other op-amps. This error affects the amplitude of voltage-time signals. Resistors with 1% tolerance are chosen throughout the system to mitigate error. The ADC introduces a quantisation error when it represents the voltages in 10-bits. A truncation error is also introduced due to rounding to 3 decimal places on the microprocessor.

Table 2: Table of Errors in the system.

Element	Element Error	Contributing Errors
Sensor	10%	Accuracy error = 10% at 50 µV
Amplifiers	0.1%	**In-Amp**: Gain Error = 0.1%
	0.0074%	**Summing Amp**: Offset Voltage Drift = 0.0024% Offset Voltage = 0.005%
Filters	0.200022%	Offset Voltage = 0.0002%, Offset Voltage Drift = 0.00002%, Resistors = 0.2%
Microcontroller	0.197%	Quantisation Error = 0.097%, Truncation Error = 0.1%

The system is modelled in LTspice. The sensor is modelled as two voltage sources (one for the electrode and one for a reference). An AC analysis was performed on the system showing the filtered bandwidth and the amplification of the system in decibels seen in Figure 4. A transient analysis is also performed to show the input range and output range into the microprocessor.

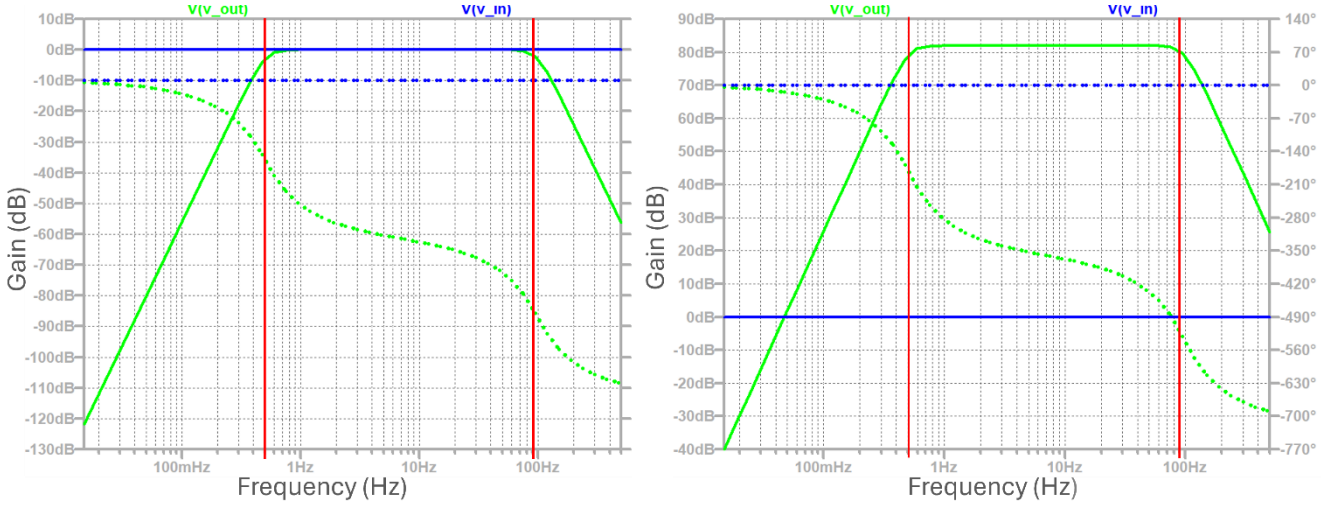

(a) Bode Plot of Filters (b) Bode Plot of System

Figure 3: Bode Plots

High-pass Transfer Function: $$H(s) = \frac{1}{(0.00000261s^2+0.001236s+1)(0.00000255s^2+0.002947s+1)} \quad (1)$$

Low-pass Transfer Function: $$H(s) = \frac{10.1796s^4}{(100000000+9.98s^2+24200s)(10000000+1.02s^2+5880s)} \quad (2)$$

System Transfer Function:

$$H(s) = \frac{127245s^4}{2.6406\times10^{-11}s^8+2.2016\times10^{-8}s^7+6.8220\times10^{-6}s^6+0.00011535s^5+0.000776019s^4+0.0024261s^3+0.0040544s^2+0.003576s+1} \quad (3)$$

These transfer functions are found using an online circuit solver [14]. The step response of the system shows a short settling time of 20 ms which would be faster than the patient would be able to process a response from the bionic prosthetic which would be required.

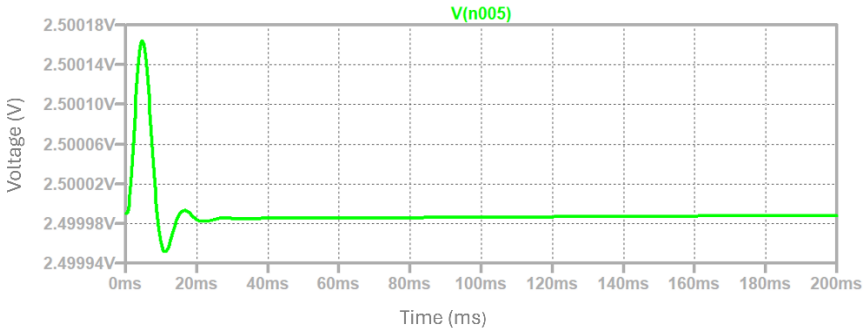

Figure 4: Step Response of the system.

5. Critical Analysis

The system has a greater error than specified by 0.50% of 10.50% error but would operate in the correct bandwidth. Operating temperatures of the operational amplifiers suggest sufficient performance through temperature ranges that the patient would experience as they are rated for much more extreme temperatures [10], [11], [12]. The total estimated cost of the components is R1000 broken down on the circuit breakdown in the appendix, and the cost of the sensor along with the surgical procedures is estimated to be R100 000 [15].The system would have a separate battery system that allows for it to be maintained easily and charged, along with all other components being modular and readily replaceable. Future improvements would be reducing the error of the system to make it more accurate as well as minimise the size of the microprocessor and possibly only use the compute chip.

5.1. Social and Ethical Impacts

This measurement system will have significant social and ethical implications. This system would be more expensive than scalp EEG systems due to the surgical costs and the more advanced technology. This would make the system less accessible to a large percentage of the population. However, this system would enable wheelchair-bound individuals facing discrimination due to their prosthetic and EEG headpiece to integrate more seamlessly into society. Due to the sub-dermal nature of the electrode, this system will have ethical concerns around the minimally invasive procedure for implantation. The accessing of neural signals is also surrounded by ethical concerns of neural hacking and disregard for the patient's autonomy [16]. The question of if it is ethical to develop a system that would only benefit those only in the upper class of paralysed people would also be of concern.

6. Conclusion

The implemented solution meets the design specifications, with only a 0.5% deviation in the total error. Following Bentley's model design, all elements are included. The system is fully simulated in LTspice, confirming performance adequacy. Cost, maintainability, and social/ethical considerations are addressed. In conclusion, this system accurately measures EEG for paralysed individuals, enabling bionic prosthetic limb use and societal integration without the need for headbands or shaved electrode sites.

BIBLIOGRAPHY

[1] I. A. Satam, "Review Studying of the Latest Development of Prosthetic Limbs Technologies," *Int. J. Sci. Eng. Res.*, vol. 12, pp. 721–731, Dec. 2021.

[2] Z. Haneef *et al.*, "Sub-scalp electroencephalography: A next-generation technique to study human neurophysiology," *Clin. Neurophysiol.*, vol. 141, pp. 77–87, Sep. 2022, doi: 10.1016/j.clinph.2022.07.003.

[3] A. Trafton, "Magnets could offer better control of prosthetic limbs," MIT News | Massachusetts Institute of Technology. Accessed: Mar. 19, 2024. [Online]. Available: https://news.mit.edu/2021/magnet-prosthetic-limb-control-0818

[4] M. Mahmoodi, B. Makkiabadi, M. Mahmoudi, and S. Sanei, "A new method for accurate detection of movement intention from single channel EEG for online BCI," *Comput. Methods Programs Biomed. Update*, vol. 1, p. 100027, Jan. 2021, doi: 10.1016/j.cmpbup.2021.100027.

[5] S. Sivakumar, "The Wave - The characteristics of an EEG," Firstclass. Accessed: Mar. 28, 2024. [Online]. Available: https://www.firstclassmed.com/articles/2017/eeg-waves

[6] E. J. Smith, "An Introduction to EEG." Accessed: Mar. 28, 2024. [Online]. Available: https://www.ebme.co.uk/articles/clinical-engineering/introduction-to-eeg

[7] V. K., D. A., M. J., S. M., A. A., and S. A. Iraj, "A novel method of motor imagery classification using eeg signal," *Artif. Intell. Med.*, vol. 103, p. 101787, Mar. 2020, doi: 10.1016/j.artmed.2019.101787.

[8] J. P. Bentley, *Principles of measurement systems*, 4th ed. Harlow, England ; New York: Pearson Prentice Hall, 2005.

[9] "15 months EEG data with UNEEG medical's subcutaneous implant." Accessed: Mar. 29, 2024. [Online]. Available: https://www.uneeg.com/implant/

[10] "AD8421 Datasheet and Product Info | Analog Devices." Accessed: May 01, 2024. [Online]. Available: https://www.analog.com/en/products/ad8421.html

[11] "ADA4523-1 Datasheet and Product Info | Analog Devices." Accessed: May 01, 2024. [Online]. Available: https://www.analog.com/en/products/ada4523-1.html

[12] "ADA4510-2 Datasheet and Product Info | Analog Devices." Accessed: May 01, 2024. [Online]. Available: https://www.analog.com/en/products/ada4510-2.html

[13] "Beston 9V 1000mAh." Accessed: May 01, 2024. [Online]. Available: https://www.gpbatteries.co.za/beston-9v-1000mah.html

[14] "Circuit Solver." Accessed: May 01, 2024. [Online]. Available: https://www.will-kelsey.com/circuitSolver/

[15] "The technology | 24/7 EEG SubQ for epilepsy | Advice | NICE." Accessed: Apr. 27, 2024. [Online]. Available: https://www.nice.org.uk/advice/mib277/chapter/The-technology

[16] S. Burwell, M. Sample, and E. Racine, "Ethical aspects of brain computer interfaces: a scoping review," *BMC Med. Ethics*, vol. 18, no. 1, p. 60, Nov. 2017, doi: 10.1186/s12910-017-0220-y.

APPENDIX

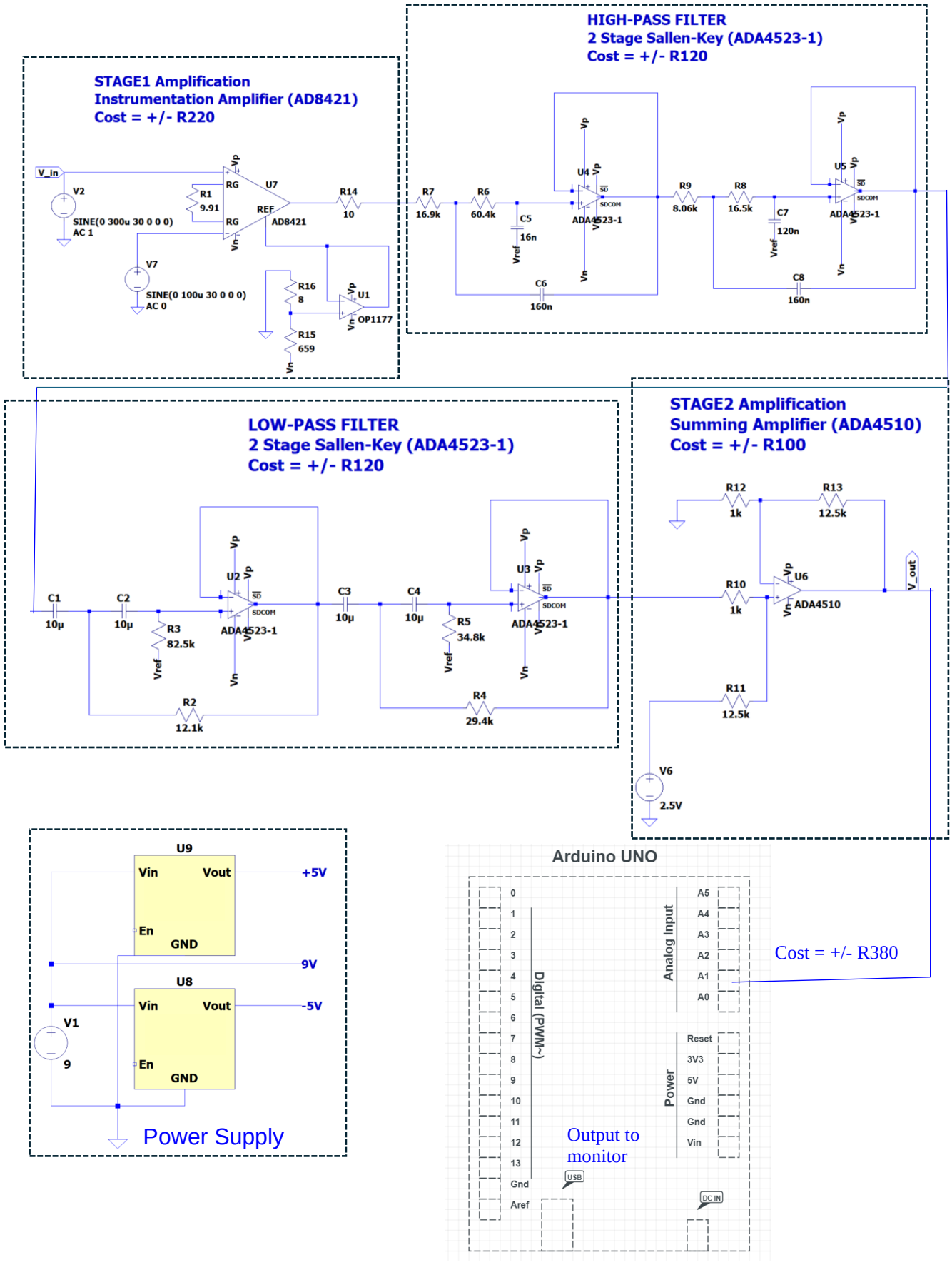

Figure 5: Complete circuit diagram of the system.